Mecánica Computacional Vol. XXIII, pp. 1471-1482
G.Buscaglia, E.Dari, O.Zamonsky (Eds.)
Bariloche, Argentina, November 2004

RECENT DEVELOPMENTS IN PATIENT-SPECIFIC IMAGE-BASED MODELING OF HEMODYNAMICS

Juan R. Cebral[*], Marcelo A. Castro[*], Rainald Löhner[*], James E. Burgess[†], Richard Pergolizzi[†], and Christopher M. Putman[†]

[*] School of Computational Sciences
George Mason University
4400 University Dr., MSN 4C7, Fairfax, Virginia 22030, USA
e-mail: jcebral@gmu.edu, web page: http://www.scs.gmu.edu/~jcebral

[†] Interventional Neuroradiology
Inova Fairfax Hospital
3300 Gallows Road, Falls Church, Virginia 22042, USA

Key words: Computational Hemodynamics, Carotid Artery, Cerebral Aneurysm, Cerebral Circulation, Endovascular Devices, Medical Images.

Abstract. *Current challenges in patient-specific computational hemodynamics include validation of the numerical models with in vivo data, the use of numerical models in large clinical studies, and the simulation of blood flow patterns in presence of endovascular devices. This paper summarizes some of the recent advances in each of these research directions. In particular, the following studies are described: validation of blood flow dynamics in carotid arteries using magnetic resonance and Doppler ultrasound, clinical study of rupture of cerebral aneurysms and relationship to intraaneurysmal flow patterns, and simulation of flow alterations into cerebral aneurysms due to implantation of stents and coils. This paper shows that accurate patient-specific hemodynamic models can be constructed from medical image data, and can be used for large clinical studies.*

1 INTRODUCTION

Stroke is the third leading cause of death after heart disease and cancer and the leading cause of long-term disability in Western world [1]. Ischemic infarction of the brain can occur due to diminution of cerebral blood flow below a certain threshold, sudden occlusion of a feeding artery, rupture of an intracranial aneurysm, embolic phenomena or surgical maneuvers.

Atherosclerotic disease of the carotid artery is a leading cause of stroke[1]. Atherosclerotic plaque in the carotid artery obstructs blood flow to the brain and stimulates the formation of thrombo-emboli that occlude downstream vessels. Unusual shear stress patterns and disturbed flows in stenotic arteries are related to plaque rupture, plaque erosion, thrombus formation and embolic phenomena.

Intracranial aneurysms are pathological dilatations of cerebral arteries. They tend to occur at or near arterial bifurcations, mostly in the circle of Willis[2]. They can be roughly classified into terminal, lateral or bifurcation aneurysms depending on their relation to the parent vessel. The most serious complication happens when the aneurysm breaks, since this has fatal consequences in 2.6 - 9.8% of the patients and serious consequences in 10.9% of the patients due to intra cranial bruise, subsequent recurrent bleeding, hydrocephaly and spasms in brain vessels [3-5]. The reasons for genesis, growth and rupture of saccular aneurysms are not clear. However, hemodynamic factors, such as wall shear stress, pressure, residence time and flow impingent, are thought to play a role in the pathogenesis of aneurysms and thrombosis [6].

Since measuring hemodynamic quantities *in vivo* is difficult, various modeling approaches have been considered in the past. *In vitro* studies allow very detailed measurement of hemodynamic variables, but cannot be used in a straight manner for clinical evaluation of individual cases. *In vivo* image-based computational fluid dynamics (CFD) models have only since recently been attempted with promising results [7-12].

In this paper, we summarize recent developments and applications of realistic patient-specific computational models of hemodynamics in normal and diseased arteries as well as blood flows in the presence of complex endovascular devices used to treat these vessels.

2 METHODOLOGY

The computational modeling pipeline used to construct patient-specific models of arterial blood flows consists in the following stages:

2.1 Vascular Model Reconstruction

Realistic patient-specific vascular models are constructed from anatomical images using deformable models. A tubular deformable model is used to construct models of normal carotid arteries [13]. This approach requires the specification of the axis of each arterial branch. This can be done manually by selection of pixels in cross-sectional views or using skeletonization procedures. A cylindrical model is then constructed along each arterial branch and deformed under the influence of internal smoothing forces and external forces derived from the image

intensity gradients [13]. The complete model is the obtained using a surface merging algorithm [14]. Although this approach works well for normal vessels which are mainly cylindrical, it tends to smooth out and underestimate stenoses. For this reason, an iso-surface deformable model [15] is used for stenosed arteries as well as arteries with aneurysms. Following this approach, the image is first smoothed by convolution with a Gaussian kernel. The voxel intensities are then sharpened. Note that the Gaussian blurring operation tends to expand the anatomical structures, while the sharpening operator tends to shrink them. The application of blurring followed by sharpening operations tends to smooth the images without shrinking or expansion of the anatomical structures. An initial reconstruction is then obtained by a region growing segmentation followed by iso-surface extraction [16]. The selection of the intensity values for these algorithms is done on a trial and error basis. As in the tubular deformable models, this surface is then allowed to deform under the action of internal smoothing forces between the connected nodes and external forces computed from the energy gradient of the original (unprocessed) image. This operation tends to place the surface nodes on the edges of the vascular structures, thus achieving sub-voxel accuracy. The final model obtained by either reconstruction technique is then smoothed using a non-shrinking algorithm [17] and vessel branches are interactively truncated and extruded in order to minimize the influence of boundary conditions on the region of interest.

2.2 Grid generation

Volumetric unstructured meshes composed of tetrahedral elements are generated using an advancing front technique [18-20]. The reconstructed model is used as a support surface, i.e. to define the geometry of the computational domain. First, an entirely new surface triangulation is generated according to an element size distribution specified by the user. The element size distribution is prescribed using analytical source functions and adaptive background grids to increase the mesh resolution in regions of high surface curvature [18]. Newly created points are positioned on the original surface by linear interpolation [21]. The volume enclosed by the surface is then filled with tetrahedral elements using the new triangulation as the initial advancing front. This approach does not require any analytical representation of the computational domain and at the same time geometric features present in the original triangulation are automatically detected and preserved in the final grid. The mesh resolution used in the present models ranged from 0.1 mm to 0.2 mm, and the finite element grids contained between 1 and 2.5 million elements.

2.3 Derivation of Physiologic Flow Conditions

Physiologic flow conditions are derived from either phase-contrast magnetic resonance (PC-MR) or Doppler ultrasound (US) measurements of flow velocity.

The PC-MR images are obtained using a neurovascular array coil on a 1.5T scanner (GE Medical Systems, Waukesha, WI). PC-MR imaging is cardiac gated by pulse oximetry and interpolated to 40 phases within the cardiac cycle. The velocity encoding gradient is set for a maximum velocity (V_{enc}) of 150 cm/sec. Only the through plane velocity component is

imaged. Images are acquired independently at each slice location. Flow rate curves are then obtained by integration of the velocity profile over the cross-section of the vessel. The lumen is segmented either manually or by thresholding of the magnitude images [22].

Carotid Duplex ultrasound images are obtained using a ATL5000 equipment (Phillips Medical Systems, The Netherlands). The ultrasound gate is adjusted to match the arterial walls. In this way, all the velocities in the lumen are sampled. Curves of maximum (peak) and minimum velocity are then identified by threshold segmentation of the ultrasound images. The mean velocity curve is computed as the average between the peak and the minimum velocity curves. These curves are then averaged over the cardiac cycle. Flow rate curves are then obtained by multiplication of the mean velocity curves by the area of the vessel lumen at the location of the US measurement. This area is obtained from the geometrical model reconstructed from the anatomical images. The area can also be estimated from measurements of the vessel diameter obtained directly from the US color Doppler image, however these measurements are not very accurate.

Fully developed velocity boundary conditions are imposed by performing a Fourier decomposition of the flow rate curves into Womersley modes [7]. Direct interpolation of the PC-MR velocity profiles to the CFD models is difficult due to the limited image resolution. Improvements of the algorithms used to impose more realistic velocity profiles are needed.

2.4 Numerical Flow Solution

Blood flow is mathematically modeled by the incompressible Navier-Stokes equations for a Newtonian fluid [10]. Non-Newtonian effects in large arteries are usually regarded as second order and neglected. However, in regions of low flow this approximation is not entirely justified and further investigation is required. For simplicity vessel wall compliance are also neglected. Fluid-structure interaction calculations accounting for wall compliance would require data on the material properties of the vessel wall, such as elasticity and wall thickness, which is difficult to obtain *in vivo*. No slip boundary conditions are prescribed at the vessel walls. Fully developed pulsatile velocity profiles are prescribed from the measured flow rate curves using a Fourier decomposition into Womersley modes. The governing equations are solved numerically using an implicit finite element formulation [23]. Since this scheme allows for arbitrary timestep sizes, typically 100-200 steps were performed in each cardiac cycle. A generalized minimum residual (GMRES) solver is used for the discretized momentum equation while a diagonal preconditioned conjugate gradient solver for the pressure equation.

2.5 Post-Processing and Visualization

The entire time-dependent flow field computed by the finite element solver is stored at every time-step. This solution is then post-processed in order to compute and visualize the studied hemodynamic variables. For instance, visualizations of the distribution of the mean (time averaged) wall shear stress magnitude (WSS), the oscillatory shear index [10] (OSI), and peak pressure are produced. Animations are constructed to visualize the distribution of intravascular flow velocities over time as a cine loop at every timestep of the second cardiac

cycle. “Virtual angiograms” are used to visualize the complex flow patterns [24]. These angiograms are constructed by solving the transport equation for a virtual dye simulating the injection of a contrast agent and calculating the time-evolution of the concentration of such dye.

3 RESULTS

3.1 Carotid Arteries

The vascular CFD methodology was validated with in vivo PC-MR velocity measurements [25-28]. The model was constructed from contrast-enhanced magnetic resonance angiography (MRA) images. Pulsatile velocity profiles obtained with the numerical models closely match the velocity profiles measured with PC-MR in the region of the carotid bifurcation of a normal volunteer as shown in Figure 1.

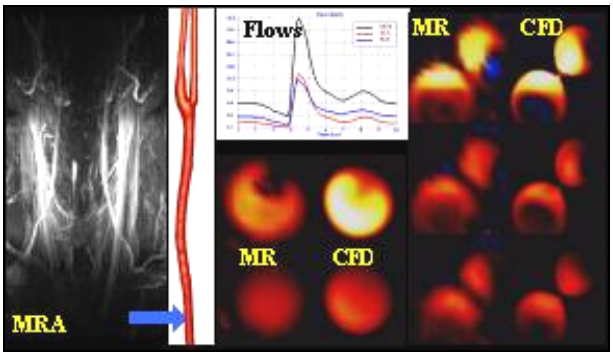

Figure 1: Comparison of CFD and PC-MR velocity profiles in the region of the carotid bifurcation of a normal subject

The methodology was also validated with multimodality image data of diseased carotid arteries [26, 27]. In this case, the models were constructed from 3D rotational angiography (3DRA) images, and flow conditions were obtained from PC-MR and Doppler ultrasound (DUS) measurements. Figure 2 shows that flow curves obtained with DUS match the flow curves obtained with PC-MR and that the computed peak velocity agrees well with the peak velocity measured at the stenosis with DUS.

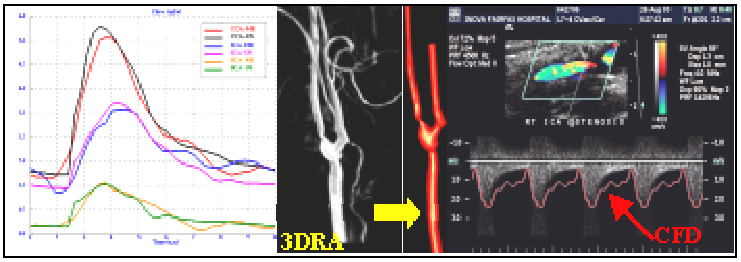

Figure 2: Comparison of CFD and DUS peak velocity at the stenosis of a diseased carotid artery.

3.2 Cerebral Aneurysms

A pilot study of the hemodynamics in cerebral aneurysm has been carried out [29]. A total of 63 aneurysm models were constructed from 3DRA images. Physiologic flow conditions were derived from PC-MR measurements in the circle of Willis of a normal subject [22]. Visualizations of the intraaneurysmal flow patterns and the distribution of hemodynamic forces on the aneurysm wall (pressure and wall shear stress) were performed. Figure 3 shows some of these visualization for 8 of the aneurysms. Based on these visualizations, the aneurysms were classified into different categories such as the complexity of the flow pattern, size of the flow impingement region, the size of the jet into the aneurysm, the location of the maximum pressure and wall shear stress, etc. Figure 4 shows examples of the four flow types defined: 1) stable, single vortex; 2) stable, multiple vortices; 3) unstable, simple; 4) unstable, complex. The aneurysms were also classified into different anatomical categories such as aspect ratio, dome and neck size, location with respect to the curvature of the parent vessel, morphology, etc.

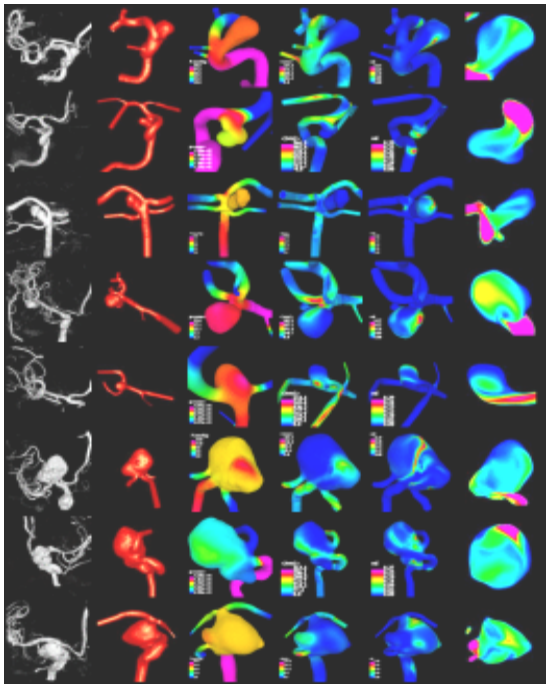

Figure 3: Examples of cerebral aneurysm models from 3DRA images and visualizations used to analyze the aneurysmal hemodynamics

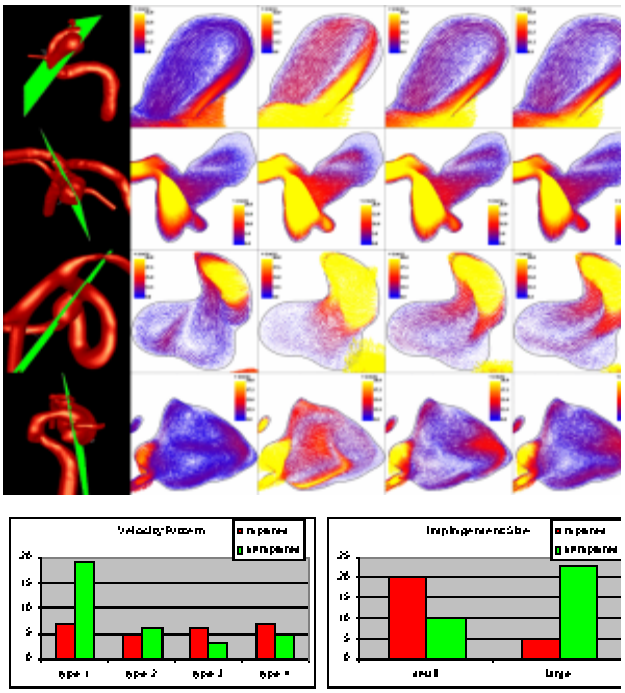

Figure 4: Examples of different intraaneurysmal flow patterns and correlations to clinical rupture data.

The number of ruptured and unruptured aneurysms in each of these categories was then counted. Although the sample studied was small to achieve strong statistical significance, the distributions of ruptured and unruptured aneurysms showed some interesting trends (see Figure 4). For instance, the majority of aneurysms with stable flow patterns were unruptured (75% for type 1 and 55% for type 2). While the majority of aneurysms with unstable flow

patterns were ruptured (60% for type 3 and 58% for type 4). The relative size of the impingement zone had a more striking difference. Figure 4 shows that 80% of ruptured aneurysms had small impingement zones accounting for 65% of aneurysms in this group. In contrast unruptured aneurysms accounted for 82% of aneurysms with large impingement zones relative to the aneurysm dome size. Only robust and efficient modeling systems will allow us to explore these interesting trends on larger datasets in a timely manner.

A preliminary sensitivity study was performed on four of the aneurysms described in the previous section. The effects of increasing the total flow, changing the flow division among the different arterial branches, using non-Newtonian viscosity models, and changing the geometry of the aneurysm were studied [30]. Figure 5 shows, from left t right, the effects of changing the viscosity model, increasing and decreasing the total flow on the distribution of wall shear stresses. Figure 6 shows the effects on the intraaneurysmal flow pattern. In this study it was found that the hemodynamic characterization of the aneurysms was not affected by changes in the total flow rates, the flow divisions, and the non-Newtonian viscosity model. It was also found that the most important factor affecting the intraaneurysmal flow pattern is the geometry of the aneurysm and the parent vessel.

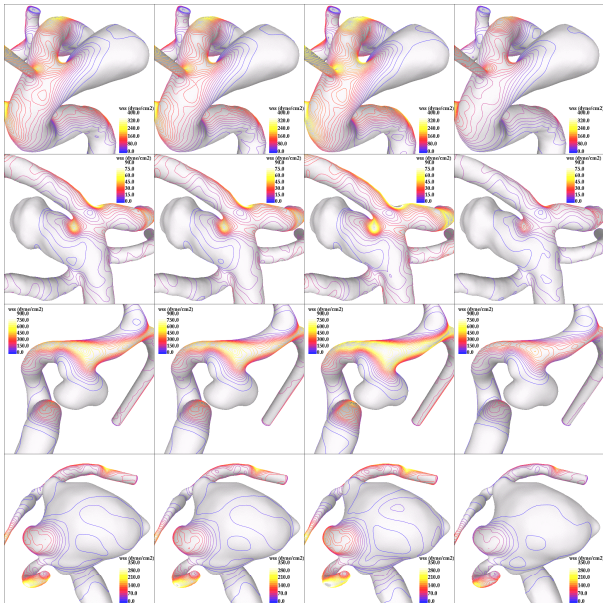

Figure 5: Sensitivity of wall shear stress distribution

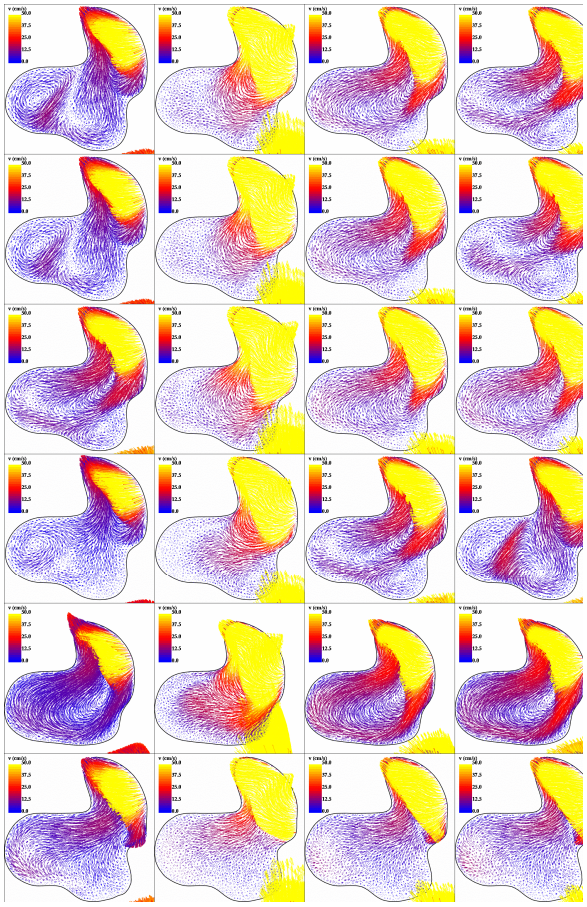

Figure 6: Sensitivity to viscosity model, flow rates and aneurysmal geometry.

In conclusion, these preliminary studies show that with our modeling pipeline clinical studies of cerebral aneurysms hemodynamics are feasible. In absence of flow information, sensitivity analyses similar to the one presented in this paper can be conducted in order to ensure a proper characterization of the intraaneurysmal hemodynamics. Special attention must be paid to obtain accurate geometrical models since the flow patterns strongly depend on the shape of the aneurysm sac.

One of the limitations of the methodology for constructing personalized models of cerebral aneurysms from 3DRA images is that aneurysms feed by more than one vessel cannot be constructed from a single image. However, multiple images can be acquired to visualize all the feeding vessels and a proper computational model can be obtained. A model of an anterior communicating artery aneurysm has been constructed from two 3DRA images obtained during contrast injection in each internal carotid artery. Two arterial models were then reconstructed from each of these images, one for the left portion of the vasculature and one for the right. The original images were then co-registered using a rigid registration, and then the same transformation was applied to the reconstructed models. The models were merged using an adaptive voxelization technique [14], and a finite element grid was generated for the entire vasculature. Figure 7 shows the stages of the model construction from the 3DRA images and the results of a CFD calculation performed assuming that the flow rates are balanced between the left and right internal carotid arteries. Obviously, these models require knowledge of the flow rates in all the feeding vessels. However, it is unknown how sensitive the intraaneurysmal flow patterns are to differences in these flow rates.

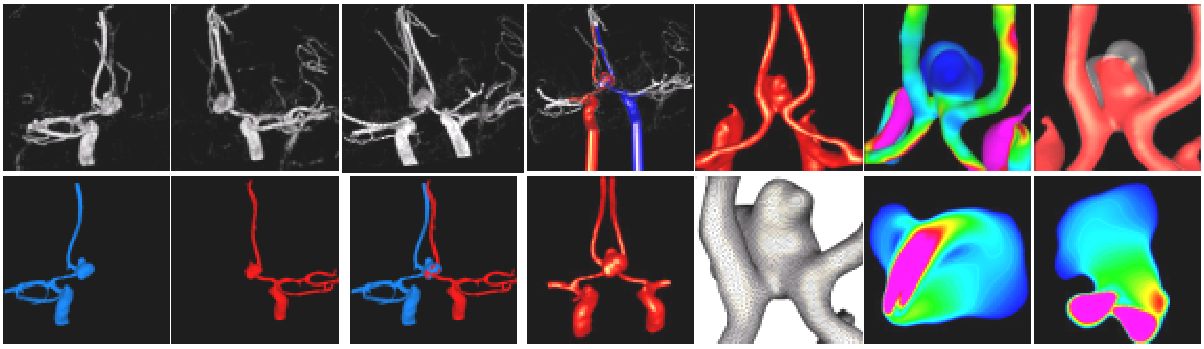

Figure 7: Model of anterior communicating artery aneurysm from two 3D rotational angiograms

3.3 Endovascular Interventions

The simulation of blood flow patterns in the presence of endovascular devices used to treat cerebral aneurysms such as coils and stents is a challenging problem due to the geometrical complexity of the devices. These devices operate by blocking the blood flow into the aneurysm and thus promoting clot formation and thrombosis, reducing the risk of future rupture. Knowledge of the intraaneurysmal hemodynamics after the implantation is useful to evaluate, optimize and personalize the treatment options (e.g. selecting the optimal amount of coils for a given aneurysm). Preliminary simulations of blood flow dynamics in the presence

of complex endovascular devices have been carried out using an adaptive embedding technique with very promising results [31]. The basic idea of this approach is to impose a wall boundary condition in the edges of the finite element grid that are intersected by the surface of the device. Coils and stents are modeled as a sequence of overlapping spheres that are then used to identify the edges of the mesh that are cut by the device. The mesh is adaptively refined in the proximity of the device surface in order to resolve the flow features around the device. Figure 8 shows an example of the flow changes that occur as a result of the implantation of a stent in an idealized aneurysm model. Figure 9 shows a simulation of the deployment of coils in an aneurysm model reconstructed from 3DRA images. This figure shows how the intraaneurysmal flow pattern changes from the pre-treatment configuration to post-treatment with a 10cm and 20cm coil. The adaptive embedding approach tremendously simplifies the simulation process of complex endovascular devices, making these techniques for the first time very attractive for clinical studies of endovascular procedures.

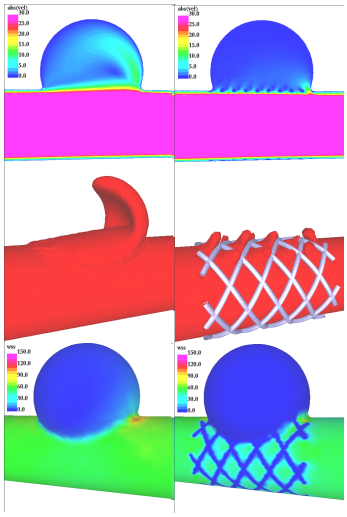

Figure 8: Idealized stented aneurysm model

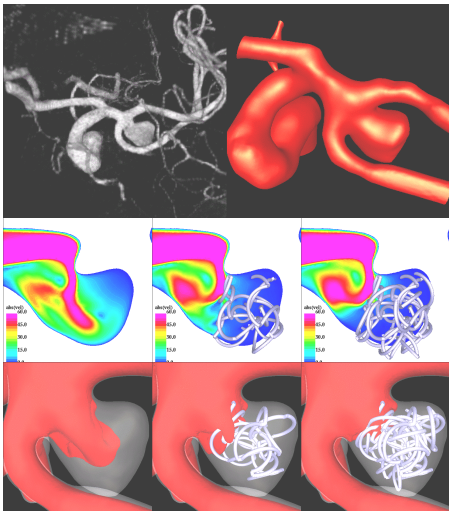

Figure 9: Patient-specific coiled aneurysm model

4 DISCUSSION

The modeling methodology has several limitations. *Wall compliance* is important for accurate calculations of peak pressures and wall shear stress distributions. Incorporating wall compliance into the numerical models requires not only coupling fluid and structural solvers but also the determination or estimation of the material characteristics of the arterial wall and the intravascular pressure waveform necessary for appropriate boundary conditions. *Non-Newtonian effects* can become relatively important in regions of low shear that are difficult to estimate a priori. *Patient-specific physiologic flow conditions* are also important for quantitative determination of hemodynamic variables. Presumably, vascular bed modes based on arterial trees [22, 32] can be used to prescribe outflow conditions that yield the correct flow divisions among the branches of a vascular model.

Despite these limitations, the methodology has been successfully applied to study the blood flow dynamics in carotid arteries from MRA images and cerebral aneurysms from 3DRA images. These models provide information otherwise inexistent on the hemodynamics conditions that are involved in the initiation and progress of vascular diseases.

The numerical models of cerebral aneurysms indicate that there are different classes of intra-aneurysmal flow patterns. Although, an exact and objective characterization of the flow patterns has not yet been attempted, the different classes of flows observed may carry different risks of rupture. It has been suggested that unstable or disturbed flow patterns induce oscillations in the aneurysm wall that may eventually lead to its rupture. The significance of this work is that these models can be used to study possible correlations between the intra-aneurysmal flow patterns and the morphology of the aneurysm and eventually with the risk of rupture.

5 CONCLUSIONS

Validation of patient-specific vascular models is difficult because there is no gold standard for measuring hemodynamic flow patterns *in vivo*. However, *in vivo* image data can be used to indirectly validate the numerical models. Comparisons of the CFD and PC-MR velocity profiles in normal carotid bifurcations show good agreement between the numerical results and the MR measurements. In addition, computed peak velocities at the stenosis of a diseased carotid artery closely match Doppler ultrasound measurements.

The use of vascular CFD models for clinical studies is limited by the efficiency of the modeling pipeline. In this paper, results for 63 aneurysm models constructed from 3DRA images were described, indicating that the modeling pipeline can be used for large clinical studies. Currently, the complete process of creating and running a patient-specific model with a mesh of around 2 million elements can be completed in a day. More automation and streamlining of the modeling processes, algorithmic improvements and optimizations will reduce these timing even further.

Modeling the outcome of medical interventions is very important in order to optimize and personalize the therapeutic options. A step forward in this direction is the modeling of endovascular devices of complex shapes such as coils and stents. The use of unstructured grid adaptive embedding techniques greatly simplifies the modeling process and provides a framework for clinical studies of endovascular interventions.

In conclusion, the results presented in this paper show that the image-based patient-specific computational methodology used to model arterial blood flows is accurate and can be used for large clinical studies.

6 REFERENCES

[1] Petty, G.W., et al., "Ischemic stroke subtypes; a population-based study of functional outcome, survival, and recurrence". *Stroke*, **31**, 1062-1068 (2000).

[2] Stehbens, W.E., *Intracranial aneurysms*. (1972).

[3] Linn, F.H., et al., "Incidence of subarachnoid hemorrhage: role of region, year, and rate of

computed Tomography: a meta-analysis". *Stroke*, **27**(4), 625-629 (1996).

[4] Tomasello, F., et al., "Asymptomatic aneurysms. Literature meta-analysis and indications for treatment". *Journal of Neurosurgical Science*, **42**(1), 47-51 (1998).

[5] Winn, H.R., et al., "of asymptomatic incidental aneurysms: re-view of 4568 arteriograms". *Journal of Neurosurgery*, **96**(1), 43-49 (2002).

[6] Kayembe, K.N.T., M. Sasahara, and F. Hazama, "Cerebral aneurysms and variations of the circle of Willis". *Stroke*, **15**, 846-850 (1984).

[7] Taylor, C.A., T.J.R. Hughes, and C.K. Zarins, "Finite element modeling of blood flow in arteries". *Computer Methods in Applied Mechanics and Engineering*, **158**, 155-196 (1998).

[8] Moore, J.A., et al., "Accuracy of computational hemodynamics in complex arterial geometries reconstructed from magnetic resonance imaging". *Annals of Biomedical Engineering*, **27**, 32-41 (1999).

[9] Zhao, S.Z., et al., "Blood flow and vessel mechanics in a physiologically realistic model of a human carotid arterial bifurcation". *Journal of Biomechanics*, **33**, 975-984 (2000).

[10] Cebral, J.R., et al., "Blood flow modeling in carotid arteries using computational fluid dynamics and magnetic resonance imaging". *Academic Radiology*, **9**, 1286-1299 (2002).

[11] Steinman, D.A., et al., "Image-based computational simulation of flow dynamics in a giant intracranial aneurysm". *AJNR American Journal of Neuroradiology*, **24**(4), 559-566 (2003).

[12] Cebral, J.R., et al. "Subject-specific modeling of intracranial aneurysms". *Proc. SPIE Medical Imaging*. San Diego, California, (2004).

[13] Yim, P.J., et al., "Vessel surface reconstruction with a tubular deformable model". *IEEE Transactions in Medical Imaging*, **20**(12), 1411-1421 (2001).

[14] Cebral, J.R., et al., "Merging of intersecting triangulations for finite element modeling". *Journal of Biomechanics*, **34**, 815-819 (2001).

[15] Yim, P.J., et al. "A Deformable isosurface and vascular applications". *Proc. SPIE Medical Imaging*. San Diego, California, (2002).

[16] Cebral, J.R. and R. Löhner, "From medical images to anatomically accurate finite element grids". *International Journal for Numerical Methods in Engineering*, **51**, 985-1008 (2001).

[17] Taubin, G. "A signal processing approach to fair surface design". *Proc. Computer Graphics*, (1995).

[18] Löhner, R., "Automatic unstructured grid generators". *Finite Elements in Analysis and Design*, **25**, 111-134 (1997).

[19] Löhner, R., *Applied CFD techniques*. John Wiley & Sons.(2001)

[20] Owen, S.J. "A survey of unstructured mesh generation technology". *Proc. 7th International Meshing Roundtable*. Sandia National Laboratory, (1998).

[21] Löhner, R., "Regridding surface triangulations". *Journal of Computational Physics*, **126**, 1-10 (1996).

[22] Cebral, J.R., et al., "Blood flow models of the circle of Willis from magnetic resonance data". *Journal of Engineering Mathematics*, **47**(3-4), 369-386 (2003).

[23] Soto, O., et al., "A stabilized edge-based implicit incompressible flow formulation". *Computer Methods in Applied Mechanics and Engineering*, **193**, 2139-2154 (2004).

[24] Calamante, F., P.J. Yim, and J.R. Cebral, "Estimation of bolus dispersion effects in perfusion MRI using image-based computational fluid dynamics". *NeuroImage*, **19**, 342-352 (2003).

[25] Cebral, J.R. "Realistic modeling of arterial hemodynamics from anatomic and physiologic image data". *Proc. 14th U.S. National Congress on Theoretical and Applied Mechanics*. Blacksburg, Virginia, (2002).

[26] Cebral, J.R., C.M. Putman, and J.E. Burgess. "Patient-specific modeling of atherosclerotic carotid arteries from multi-modality image data". *Proc. IMECE*. Washington, DC, (2003).

[27] Cebral, J.R., et al. "Multi-modality image-based models of carotid artery hemodynamics". *Proc. SPIE Medical Imaging*. San Diego, California, (2004).

[28] Yim, P.J., et al. "Estimation of mechanical stress on the carotid artery". *Proc. Biomedical Engineering Society (BMES)*, (2001).

[29] Cebral, J.R., et al., "Characterization of cerebral aneurysm for assessing risk of rupture using patient-specific computational hemodynamics models". *AJNR American Journal of Neuroradiology*, **submitted** (2004).

[30] Cebral, J.R., et al., "Efficient pipeline for image-based patient-specific analysis of cerebral aneurysm hemodynamics: Technique and sensitivity". *IEEE Transactions in Medical Imaging*, **accepted for Special Issue on Vascular Imaging** (2004).

[31] Cebral, J.R. and R. Löhner, "Efficient simulation of blood flow past complex endovascular devices using an adaptive embedding technique". *IEEE Transactions in Medical Imaging*, **accepted for Special Issue on Vascular Imaging** (2004).

[32] Cebral, J.R., R. Löhner, and J.E. Burgess. "Computer simulation of cerebral artery clipping: relevance to aneurysm neuro-surgery planning". *Proc. ECCOMAS*. Barcelona, Spain, (2000).